ILASS-Americas 22nd Annual Conference on Liquid Atomization and Spray Systems, Cincinnati, OH, May 2010

Morphology of Diesel Sprays from Single-Orifice Micronozzles

Jian Gao[1,2], Zunping Liu[1], Seoksu Moon[1], Xingbin Xie[3], Eric Dufresne[1], Kamel Fezzaa[1], Ming-chia Lai[3], Jin Wang[1*], and Rolf D. Reitz[2]

[1]Advance Photon Source, Argonne National Laboratory, Argonne, IL 60439
[2]Engine Research Center, Department of Mechanical Engineering, University of Wisconsin-Madison, Madison, WI 53706
[3]Mechanical Engineering Department, Wayne State University, Detroit, MI 48202

Abstract

Ultrafast (150 ps) X-ray propagation-based phase-contrast imaging technique was used to obtain high-spatial-resolution, single-shot images of the dense diesel fuel jets in the near-nozzle region (0∼6 mm) issuing into a quiescent nitrogen gas ambient. Specially fabricated axial single-hole nozzles with diameters of 135 and 96 micrometers were used to inject both commercial diesel and biodiesel at different injection pressures. The injection pressure of the fuel jet was varied between 30 and the 100 MPa while the entire injection process and the breakup of the fuel jet was investigated in the optically dense near-nozzle region. From a slightly hydroground micronozzle, the near-nozzle jet showed the transition of laminar to turbulent flow within a few millimeters from the nozzle exit depending on the injection conditions during the quasi-steady flow state. For a similar micronozzle with a smaller orifice diameter and a rather sharp entrance to the orifice, the jet morphology exhibits the typical properties of turbulent primary breakup. The validity of Ohnesorge classification on round jet breakup was also studies to understand this breakup phenomenon. These results will undoubtedly facilitate better understanding the atomization mechanisms of liquid jets and provide directly experimental evidence for high-fidelity computations and simulations.

*Corresponding Author: wangj@aps.anl.gov

Introduction

Liquid jets and sprays are encountered in nature as well as in various industrial applications, such as waterfall mists, garden hoses, food processing, film coating, agricultural spraying, ink jet printing, gas-liquid mass transfer applications, spray combustion, etc. [1, 2]. Specifically, liquid sprays are commonly used to disperse liquid fuels for combustion in internal combustion engines, gas turbines, rocket engines, and industrial furnaces which is dependent on effective atomization to increase the specific surface area of the fuel and thereby achieve high rates of mixing and evaporation. In most DI diesel engines, reduction in mean fuel drop size leads to higher volumetric heat release rates, easier lightup, a wider burning range, and lower exhaust concentrations of pollutant emissions [3].

The liquid jet atomization, at least in low-pressure case, consists of two distinctive subprocesses: primary and second breakup. The primary breakup process refers to droplet formation through stripping from the liquid surface, which controls the initial droplet size distribution and velocity [4, 5]; while the secondary breakup is known as the droplets so formed further disintegrate into droplets of smaller size if they exceed the critical size. It is well recognized that the primary breakup has a predominant impact on the fuel evaporation, mixture formation, and the whole combustion process. However, its physics is still not well understood, due not only to its complexity and transient nature, but also to the very high optical density in the near-nozzle field (inaccessible by conventional laser-based diagnostics).

Recently, with the high-energy and high-brilliance X-rays available at the third-generation synchrotron sources in Argonne National Laboratory, X-ray radiography and phase-contrast imaging have been used to study the high-speed diesel spray [6, 7]. Owing to the weak interaction of X-rays with matter, the X-ray imaging technologies have shown the ability to elucidate the interior structure and dynamics of the spray with high temporal and spatial resolutions, especially in the near-nozzle field.

The breakup of a liquid jet is not completely understood because of the complexity of the breakup process which is due to the unusually large number of parameters which influence it, including the details of nozzle geometry, the jet's velocity and turbulence, and physical and thermodynamic states of both liquid and gas. There is still no comprehensive theoretical framework to model the jet disintegration and breakup, especially, in high-injection pressure region. The main shortcomings of existing theories are due to the influence of the nozzle geometry on jet breakup is generally ignored. Experimental data is crucial to developing and validating any all-inclusive models that may appear in the future [3].

The current work is therefore an effort to visualize the near-nozzle morphology (0∼6 mm) and to better understand the primary breakup process of diesel sprays (link to the nozzle internal structure) using the ultrafast X-ray phase-contrast imaging technique. We focus on the simplest and ideal case, viz. the cylindrical jet emanated from a single circular orifice issuing into the quiescent gas ambient. The jet structures during the quasi steady state, in particular the jet morphology and primary breakup process were examined and analyzed.

Experimental Methods

The X-ray imaging experiment was carried out at the XOR 7-ID-B beamline of the Advanced Photon Source (APS) at Argonne National Laboratory. As shown in Fig. 1, the X-ray beam was generated from the APS electron storage ring with a hybrid-singlet fill pattern, in which a single electron pulse (150 ps long) was separated from a train of electron bunches (472 ns long) by a 1.59 μs gap on both sides. With the undulator gap set to 20 mm, most of the intensity was located within the first harmonic at ∼10 keV. The X-ray beams were chopped by a millisecond shutter and a microsecond shutter at a rate of 1 Hz, reducing the heating power of the beam by more than 99%. Then the beams passed through the spray. The spray chamber was located 40 m downstream from the source. The transmitted and diffracted X-rays were converted into visible light by a fast-scintillator crystal, and were captured with a fast gated CCD camera coupled with a microscope objective lens (10×) and a 45^o mirror.

A common-rail injection system and specially fabricated solenoid-actuated injectors with single-orifices were used to inject diesel fuel into a quiescent nitrogen gas ambient. The spray chamber features a gentle flow of the nitrogen gas (at atmospheric pressure and room temperature) to scavenge the fuel vapors. The shutters, CCD camera, and injection system were synchronized to the X-ray pulses. The field of view of the imaging system was 0.66×0.88 mm^2 with a spatial resolution of 0.64 μm/pixel. The pulsed nature of the X-ray beam combined with an adequate shuttering and timing of the setup provided an effective exposure time of 150 ps for each image.

The contrast in the recorded images with this propagation-based imaging technique comes from a phase effect [7, 8]. This contrast depends on the

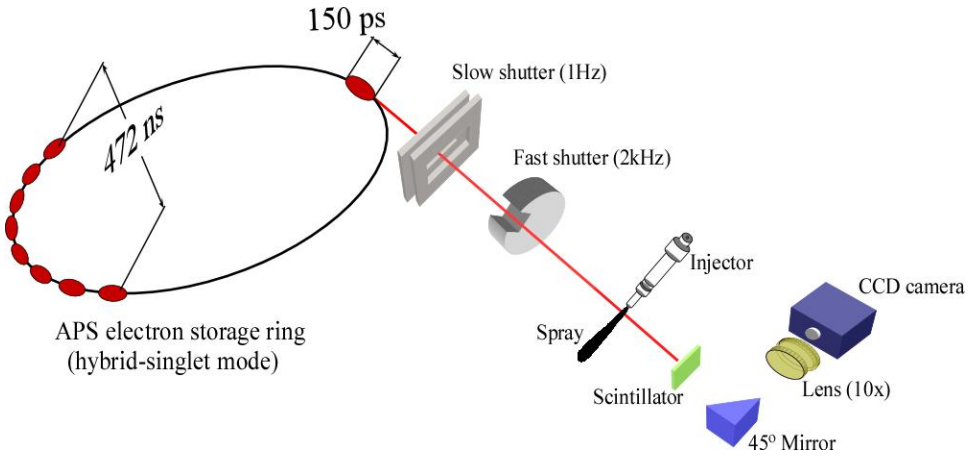

Figure 1: Schematic diagram of the experimental setup for X-ray phase-contrast imaging.

Nozzle	Single-orifice (d_0=0.135 mm, L/d_0=6.0)	Single-orifice (d_0=0.096 mm, L/d_0=8.3)
ρ_f (kg/m^3)	888 (biodiesel), 855.5 (No.2 diesel)	
ν_f $(cSt)@40^oC$	4.4 (biodiesel), 2.9 (No.2 diesel)	
σ_f $(N/m)@40^oC$	0.033 (biodiesel), 0.028 (No.2 diesel)	
ρ_g	1.145	
p_{inj} (MPa)	30-90	
u_0 (m/s)	210.3-400.0	193.4-367.0
Re_{fd}	7,900-32,500	5,300-16,800
We_{gd}	240.0-879.1	144.0-528.6
We_{fd}	175,800-632,800	109,700-95,000
Oh_d	0.0245-0.0549	0.035-0.0626

Table 1: Test conditions.

Laplacian of the phase shift undergone by the beam upon its passage through the sample. Therefore, the contrast is most sensitive to boundaries and interfaces between materials with different refraction index or abrupt thickness variations, which are greatly enhanced.

The image processing was carried out using Matlab software. For the acquired X-ray images, each image was normalized by the background image and further Gaussian filtered to even out background intensity, increase contrast, and eliminate imperfections in the optics. Background images were recorded prior to injection, and also averaged.

Test Conditions

Two specially fabricated diesel nozzles with axial single-orifice were used. The nominal hole diameter was 0.135 and 0.096 mm, respectively. Hereafter, they are referred to as: SH0135 and SH0096. The hole length for both nozzles was 0.8 mm. X-ray imaging was also carried out to visualize the nozzle internal structure, and the results will be discussed in the following section.

Test conditions for both nozzles are summarized in Table 1. Both biodiesel and No.2 diesel were used as the injection fuel. The injection energizing time was set to 3 ms for all test cases so that the entire injection process and the breakup of the fuel jet can be investigated at quasi-steady flow state. The injection pressure of the fuel jet was varied between 30 and the 100 MPa, leaving the jet velocity in the range 200-400 m/s. The experimental conditions yield the following ranges of jet and primary breakup dynamic parameters: Re_{fd} of 5300-32,500, We_{gd} of 140-880, We_{fd} of 100,000-630,000, Oh_d of 0.0245-0.0625.

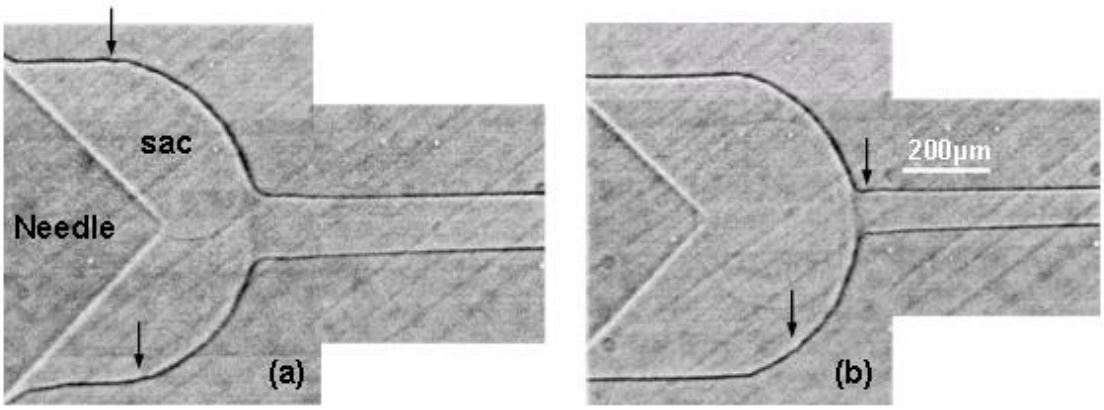

Figure 2: Nozzle internal structure captured by X-ray phase-contrast images. (a) d_0=0.135 mm, L/d_0=6.0; (b) d_0=0.096 mm, L/d_0=6.0.

Results and Discussion

Nozzle internal structure

The internal geometries of both test nozzles are imaged [9] in Fig. 2. A careful examination of the images shows that the sac structures of the two nozzles are slightly different (the sac volume of SH0135 nozzle is somewhat smaller than that of SH0096), but the measured hole diameters are quite close to the specified values. In addition to the different hole diameter, the images also indicate that the inlet of SH0135 nozzle is ground resulting in slightly round corners, while the SH0096 nozzle has undergone very little hydrogrinding, leaving a rather sharp entrance to the orifice. It is expected that these differences in the nozzle internal geometry can lead to a different near-nozzle morphology and primary breakup process, shedding some light on the liquid jet atomization mechanisms. In addition, some fabrication imperfections in the nozzle interior are also clearly revealed in Fig. 2 as indicated by the arrows.

Near-nozzle morphology and primary breakup process of SH0135 nozzle under various injection conditions

Figures 3 and 4 show the X-ray phase-contrast images of biodiesel and diesel sprays from the SH0135 nozzle at various injection pressures. The images were taken at 2.5 ms after start of injection, when the flow was considered at the quasi-steady state (the needle is in full lift at 900 bar injection pressure). Image frames taken at different distances from the nozzle exit were stitched together to give an overall view of the primary breakup process (frames were not taken concurrently). In sharp contrast to conventional laser-based imaging measurements, the internal features of the spray, like morphology and dynamics, are clearly visualized in the X-ray phase-contrast images with ultrahigh spatial resolution.

During the quasi-steady flow, the jets discharged from the SH0135 nozzle show a columnar shape, and possess a very smooth morphology in the very near nozzle region, suggesting that they remain as a liquid column rather than breaking into ligaments or droplets. Under certain conditions (p_{inj} >700 bar for biodiesel, >300 bar for diesel), wavy structures are observed on the liquid surface, indicating the transition of laminar to turbulent flow. Further downstream, the jet exhibits a complex internal structure because of turbulence in the flow, and therefore is considered to become fully turbulent. At the turbulent region, ligaments are formed and peeled from the liquid surface with no preferential direction. Additionally, in all cases, the jets have a crease-like appearance on the intact liquid surface and beyond.

As shown in Figs. 3 and 4, with the increase of injection pressure, the appearance of wavy structure on the liquid surface moves toward the nozzle exit, and thus the intact surface length of the jet decreases for both liquids. The flow patterns of the SH0135 nozzle are very similar to another hydroground nozzle that was tested previously [10], where the patterns are independent on ambient gases. Since the jet at low injection pressures (300 and 500 bar) in Fig. 3 appears as laminar-like flow, the jets issued from the SH0135 nozzle are considered to be initially nonturbulent. The round corners of the orifice inlet allow the fuel to better stream into the nozzle, and suppress the separation effect and cavitation. The injector passage vorticity mechanism for nonturbu-

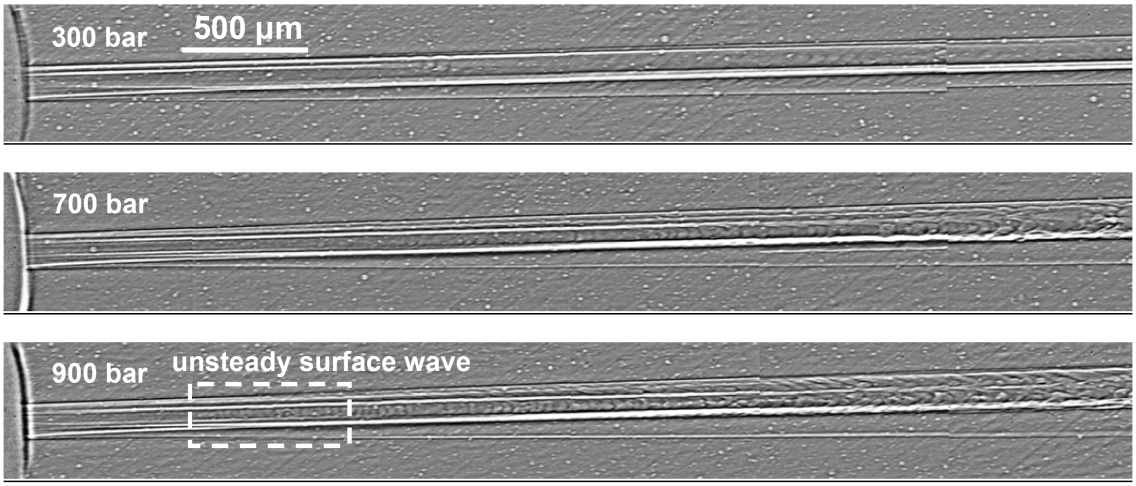

Figure 3: Biodiesel sprays in the near-nozzle field at quasi-steady state (2.5 ms after start of injection) under various injection pressures for SH0135 nozzle.

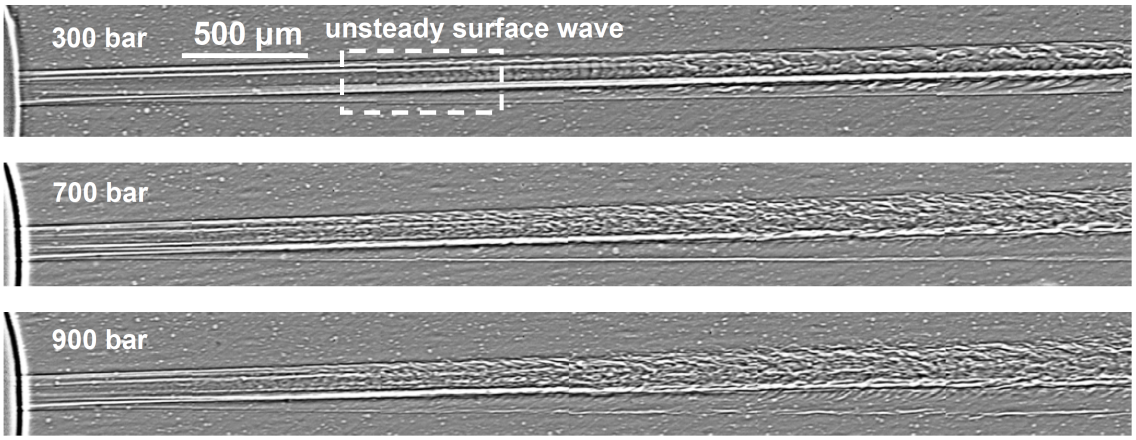

Figure 4: Diesel sprays in the near-nozzle field at quasi-steady state (2.5 ms after start of injection) under various injection pressures for SH0135 nozzle.

lent jets proposed by Wu et al. [11] may be responsible for the surface wave formation and therefore dominate the primary breakup process.

The jet morphologies from the near-nozzle field of both liquids at the same operating point are also significantly different. For instance, at the injection pressure of 500 bar, the biodiesel jet appears to be laminar-like flow, while the surface waves have obviously developed for the diesel jet, and the jet shows the transition of laminar to turbulent flow. The only factor that can explain this phenomenon is the physical properties, such as the liquid surface tension, density, and viscosity.

Near-nozzle morphology and primary breakup process of SH0096 nozzle under various injection conditions

Figures 5 and 6 show the images of biodiesel and diesel sprays from the SH0096 nozzle during the quasi-steady flow state at various injection pressures. The injection conditions remained same to that for the SH0135 nozzle. It can be seen that the jet morphology is very different to that from the SH0135 nozzle. The flow exhibits the typical properties of turbulent primary breakup as observed by [11, 12]. Regardless of the test liquids and injection pressure, the liquid surface just becomes roughened very close to the jet exit and does not breakup within the distance of a few hole diameters. Then the scale of sur-

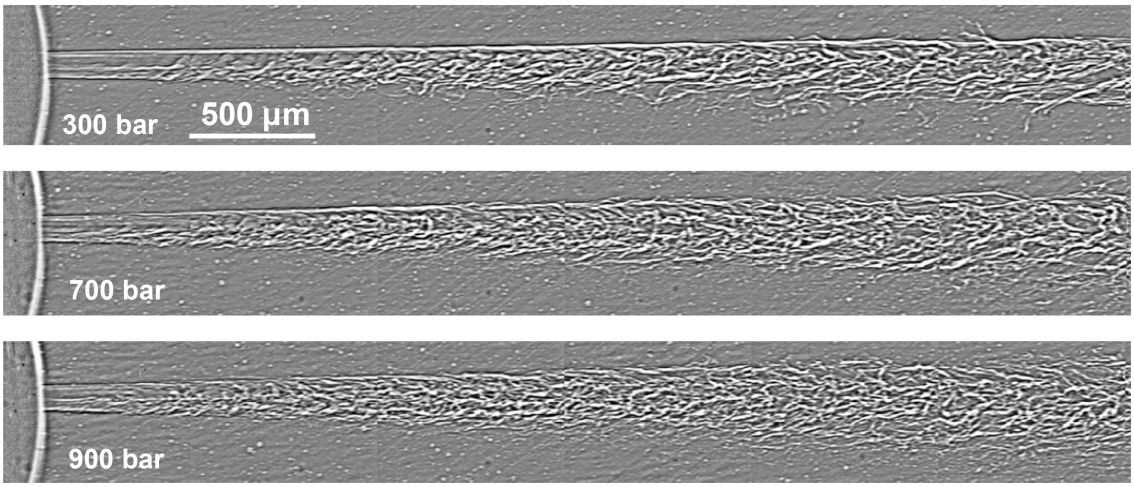

Figure 5: Biodiesel sprays in the near-nozzle field at quasi-steady state (2.5 ms after start of injection) under various injection pressures for SH0096 nozzle.

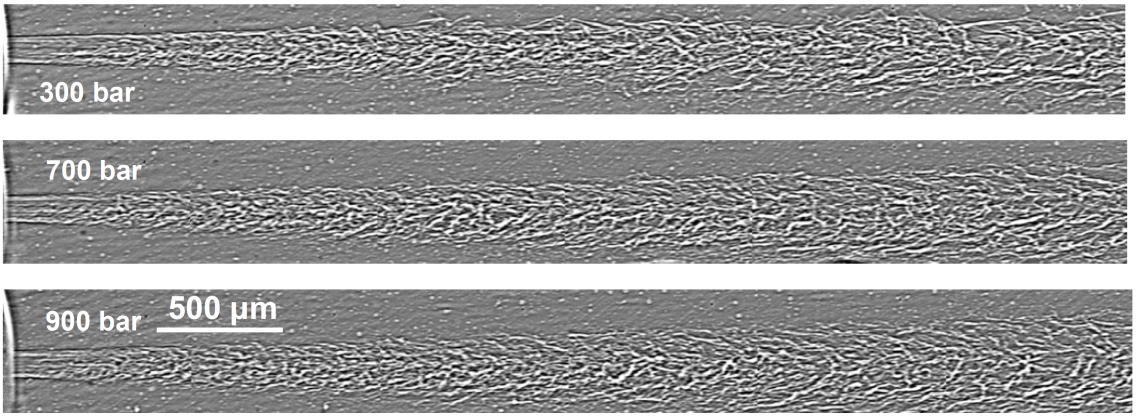

Figure 6: Diesel sprays in the near-nozzle field at quasi-steady state (2.5 ms after start of injection) under various injection pressures for SH0096 nozzle.

face distortions increases progressively with increasing distance from the jet exit, and the bulk of the jet eventually break up into large ligaments within 1 mm downstream for all test cases. It is noted that the onset of breakup always occurs on the bottom side, and the jet structure is rather asymmetric. In addition, with the increase of injection pressure or lower liquid viscosity, the average ligament size decreases.

It is speculated that the turbulent primary breakup of the SH0096 nozzle is dominated by the initial turbulence-related disturbances created within the nozzle (probably only on the bottom side). This could be stronger geometry-induced turbulence (smaller hole diameter), cavitation within the hole (sharp inlet as shown in Fig. 2 b), or greater wall friction (larger L/d), although it is impossible to distinguish them from the current results. We attribute the asymmetry to asymmetry of nozzle orifice due to variation of surface finish or degree of grinding.

Finally, all of the results presented above are summarized and compared to the most commonly accepted jet disintegration classification in the fluid mechanics literature, viz. the Ohnesorge classification [13, 14], as shown in Fig. 7. The classification argued that four distinct regimes of round jet breakup can be identified on a log-log plot of liquid Oh number versus liquid Re number. The boundaries of the regimes are represented by oblique lines with negative slope on the log-log plot. For a given nozzle (approximately constant Oh), when increas-

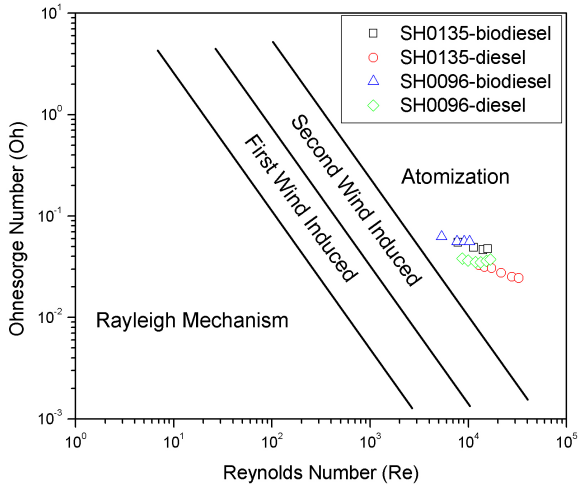

Figure 7: Ohnesorge classification of the modes of round jet disintegration [15, 16] and the test conditions in this study.

ing the jet velocity (Re) the jet breakup will in turn experience the so-called Rayleigh capillary mechanism region, first wind induced region, second induced region, and atomization region. As mentioned earlier, test conditions in this study place the measurements for both nozzles in the atomization region where the breakup essentially occurs at the nozzle exit. The jets issued from the SH0096 nozzle are atomized very close to the nozzle exit as predicted by Ohnesorge theory while the one discharged from the SH0135 does not. The observation confirms the concern raised by Lin and Reitz [4] about the shortcomings of the Ohnesorge theory that does not include the effect of the initial state of the jet (that is influenced, for example, by the nozzle internal structure).

Conclusions

Morphology and primary breakup process of fuel sprays from single-orifice micronozzles were studied in the near-nozzle region, considering biodiesel and diesel jets in quiescent nitrogen at atmospheric pressure. By using ultrafast X-ray phase-contrast imaging technique, high-spatial-resolution, single-shot images of the optically dense fuel jets were obtained and analyzed during the quasi-steady state.

The results show that the jet morphology is highly sensitive to nozzle internal geometry. The very little difference of nozzle inlet shape by the hydrogrinding process may lead to a striking different primary breakup property in the near-nozzle region. The near-nozzle spray showed the transition of laminar to turbulent flow within a few millimeters from the nozzle exit. In the meantime, wavy structures were observed on the liquid surface. At the turbulent region, ligaments are peeled from the liquid surface with no preferential direction when the surface wave breaks up. The scale of surface distortions increases progressively with increasing distance from the jet exit, and the bulk of the jet eventually break up into large ligaments for all test cases. Finally, the validity of Ohnesorge classification on round jet breakup was tested, which does not agree well with the data.

Future work will involve systematically investigating the role that the internal geometry of injection micronozzles plays in primary breakup process. Quantitative analysis of surface wave growth and comparisons with theoretical prediction are also underway.

Acknowledgments

This work and the use of the APS at Argonne National Laboratory were supported by the U. S. Department of Energy (DOE), Office of Science, Office of Basic Energy Sciences, under Contract No. DE-AC02-06CH11357. The work is partially supported by DOE Office of Vehicle Technology. The authors would like to thank Denso Corp. and Nippon Soken Inc. for providing the injectors and technical support.

References

[1] A. W. Lefebvre. *Atomization and Sprays*. Hemisphere Publishing Corporation, New York, 1989.

[2] S. P. Lin. *Breakup of Liquid Sheets and Jets*. Cambridge University Press, Cambridge Unite Kingdom, 2003.

[3] M. Birouk and N. A. Lekic. *Atomization and Sprays*, 19:501–528, 2009.

[4] S. P. Lin and R. D. Reitz. *Annu. Rev. Fluid Mech.*, 30:85–105, 1998.

[5] G. Smallerwood and O. L. Gulder. *Atomization and Sprays*, 10:355–386, 2000.

[6] J. Wang. *Journal of Synchrotron Radiation*, 12:197–207, 2005.

[7] Y. Wang et al. *Nature Physics*, 4:305–309, 2008.

[8] S. W. Wilkins et al. *Nature*, 384:335–338, 1996.

[9] W. K. Lee, K. Fezzaa, and J. Wang. *Applied Physics Letters*, 87:084105–1–084105–3, 2005.

[10] Z. P. Liu. *11th International Conference on Liquid Atomization and Spray Systems*, Vail, Colorado USA, July 2009.

[11] P. K. Wu, R. F. Miranda, and G. M. Faeth. *Atomization and Sprays*, 5:175–196, 1995.

[12] K. A. Sallam and G. M. Faeth. *AIAA Journal*, 41:1514–1524, 2003.

[13] C. C. Miesse. *Indust. Engng. Chem.*, 47:1690–1701, 1995.

[14] W. Ohnesorge. *Z Angew. Math. Mech.*, 16:355–358, 1936.